Investigation of the Elastic Properties of Dense Ceramics of the Binary System Al_2O_3-ZrO_2 after Thermal Shocks

N. Traon, T. Tonnesen, G. D. Franca, P. Piccolo, R. Telle

The work herein correlates elastic properties and microstructural characterization of dense ceramic materials elaborated by slip casting before and after thermal shocks in water. A total of eleven formulations of the binary system Al_2O_3–ZrO_2 are studied. Therefore a partially stabilised zirconia doped with 3 mol.-% of yttria with a limited quantity of monoclinic phase is used to avoid undesirable microstructure damaging during the sintering of the ceramic samples at 1550 °C/3h. The quenching cycles in water are progressively performed according to DIN 51068 at 400 °C to examine the lonely influence of the crack initiation on the microstructural and elastic properties of the samples. Young's modulus, damping properties of the flexural resonant frequency and the non-linearity of the flexural resonant frequency are determined through Resonant Frequency Damping Analysis via the Impulse Excitation Technique at room temperature after each thermal shock cycle according to ASTM C 1548-02. Scanning Electron Microscopy (SEM) completes this survey in order to understand the elastic property changes of these ceramic pieces after damaging in regard to their microstructural changes. This study aims to gather fundamental knowledge with regard to internal friction phenomena in the binary system Al_2O_3–ZrO_2. Indeed such a data acquisition leads to a better understanding of the evolution of the elastic properties of typical high alumina refractory formulations with addition of partially stabilised zirconia.

1 Introduction

The estimation of the service life of refractory materials through thermal shock tests constitutes a central point of investigation [1]. Therefore, the evaluation of the retained elastic properties of such materials is particularly appreciated as a non-destructive testing method [2–4]. Resonant Frequency Damping Analysis (RFDA) and more generally the assessment of the retained material stiffness turns out to provide essential information with regard to the elastic behaviour of refractory materials after progressive thermal shocks [5, 6]. The acquisition of both flexural and torsion frequencies enables the determination of the Young's modulus and the shear modulus respectively by implementing the geometry of the sample. From both properties an estimation of the Poisson's ratio is possible. Such a property has however, no significant relevance after thermal shock tests and just contributes to stress the anisotropy of the material structure. The examination of the damping behaviour of the resonant frequencies through RFDA provides further information concerning the friction phenomena occurring in the microstructure after mechanical excitation. Such an examination has to be correlated with the microstructure of ceramic materials. Young's modulus and damping in correlation with microstructure examination lead to a joint estimation of the material damaging, once characterising the crack network throughout the microstructure.

Design of new formulations with the aim of improving the thermal shock resistance and hence the service life of refractory shapes during application is a prominent purpose.

Nicolas Traon, Thorsten Tonnesen, Rainer Telle
GHI/RWTH-Aachen
Institute of Mineral Engineering
Department of Ceramics and Refractory Materials
52064 Aachen
Germany

Gabriela Diniz Franca
Pontificia Universidade Catolica de Minas Gerais
Belo Horizonte (MG) 31270-901
Brazil

Pierluigi Piccolo
Federal University of Rio de Janeiro
Rio de Janeiro (RJ) 21941-901
Brazil

Corresponding author: *Nicolas Traon*
E-mail: traon@ghi.rwth-aachen.de

Keywords: thermal shock, impulse excitation technique, partially stabilised zirconia, Young's modulus, damping, non-linearity

Received: 28.05.2015
Accepted: 08.06.2015

As crack initiation cannot be avoided during application, additives are incorporated into standard formulations to enhance toughening mechanisms that aim to counter the crack propagation and preserve the mechanical and structural integrity of the material. Within this framework, partially stabilised zirconia is a common oxide used for the beneficial impact of its martensitic transformation [7, 8]. Indeed such an oxide presents two different lattice structures up to traditional service temperature in steel and metallurgical applications. The monoclinic structure is stable at low temperature up to the martensitic transformation at 1170 °C onto tetragonal form. During the reversible transformation, the considerable volume expansion from 3 to 5 % constitutes the major crystallographic criterion as basis for toughening property. The energy of the crack propagation can induce the transformation of the stabilised tetragonal particles into monoclinic ones and the ensuing volume expansion of the particle causes the partial crack closure and also formation of microcracks in the surrounding areas of the zirconia particles that can also absorb a part of the energy of the main crack network [9]. The understanding of such toughening mechanisms in heterogeneous refractory materials through Resonant Frequency Damping Analysis needs the understanding of those mechanisms in dense materials. Roebben et al. reported the high damping capacity of partially stabilised zirconia during the martensitic transformation after performing in situ high temperature damping measurements up to 1000 °C [10]. By assuming a negligible apparent porosity in those dense materials, the examination of the damping behaviour in correlation with the microstructure characterization may constitute a solid data base to better understand the friction phenomena at the grain boundaries between zirconia particles and alumina particles and to provide a thorough interpretation of the damping behaviour in traditional refractory material formulation containing zirconia. By studying the whole spectrum of the binary system Al_2O_3-ZrO_2, this survey aims to examine the influence of the nature of the interface between the particles on the damping behaviour. Indeed, by adding some alumina to a pure zirconia formulation, the contact surface between alumina particles and zirconia particles increases until alumina becomes the major phase of the system. Thus, each configuration with regard to the nature of the interface can be examined: zirconia/zirconia, zirconia/alumina and alumina/alumina. After the necessary excitation of the sample for the acoustic signal development, those three interfaces can be submitted to internal friction phenomena. In such a tribological context, two parameters have to be taken into consideration: the distance between the crack flanks, which can be described as the local mean crack width, and the nature of the particles situated at the level of the cracks. Thus, to generate the damping of the acoustic signal, the crack width should be as low as possible to favour the friction phenomena. Besides, the nature of the particles can influence this tribological background. Parasibu studied the friction and wear of zirconia and alumina ceramics doped with CuO. In addition to external parameters that can influence the coefficient of friction between two materials, namely the nature of the atmosphere, the air moisture, the magnitude of the load applied on the material, the sliding velocity or the presence of lubricating agent, Parasibu proved that under comparable experimental conditions, the coefficient of friction of alumina in contact with alumina is much lower than that of alumina in contact with zirconia [11]. This experimental observation proves that the addition of zirconia in a pure alumina system will result in increasing the friction intensity. Therefore, it can be assumed that the friction phenomena occurring at the interfaces between zirconia particles is more considerable than those occurring at the interfaces between zirconia and alumina particles, which are also more considerable that those taking place at the interfaces between alumina particles.

This study focusses on the local friction phenomena taking place at microscopic scale between alumina and zirconia particles in order to better understand the role of each phase in the damping behaviour of the specimen. The extension of the results of the study beyond those experimental conditions should be subjected to careful scrutiny and critical analysis, namely concerning the possible extension to refractory materials. Indeed such heterogeneous materials exhibit a non-negligible apparent porosity (around 20 %). Those pores, which can be located at the grain boundaries of alumina or zirconia grains, can influence the local friction properties between the particles. Moreover, coarser grains (up to 6 mm) are commonly used for typical refractory formulations. In that case, after progressive thermal shocks, cracks are propagating throughout the matrix by separating pure zirconia grains from a pure alumina matrix. This microstructural observation is not comparable with the random distribution of fine particles of zirconia and alumina on both sides of the crack that can be noticed within the framework of this survey.

In the following study, quenching tests in water are performed at 400 °C in agreement with Hasselman's theory in order to limit the crack initiation at its early stage and to focus on this damaging step of the material [12]. Three thermal shock cycles are performed on each formulation but this survey highlights the evolution of the elastic properties of ceramic materials of the binary system Al_2O_3–ZrO_2 after the first quenching test to neglect the effect of crack propagation and crack unification.

A part of the study is dedicated to the non-linearity of the acoustic response of the materials after excitation. In presence of defects, namely cracks and microcracks, induced by progressive thermal shocks, the resulting acoustic signal of ceramic pieces is assumed to exhibit a non-linear behaviour [13, 14]. In such experimental conditions, which suppose a low density of cracks propagating in a dense matrix, the treatment of the non-linearity of the acoustic response may provide further information concerning the nature of the damaging in agreement with the microstructure examination and in an optimal case may justify the damping behaviour of the ceramic pieces.

2 Experimental procedure

2.1 Material and thermal shocks

Eleven formulations of the binary system Al_2O_3–ZrO_2 are defined to provide better coverage of this system. Therefore, reactive alumina CT 3000 LS SG (D_{50}: 0,780 µm) provided by Almatis and a partially stabilised zirconia, doped with 3 mol.-% of yttria, TZ-3YS-E (D_{50}: 0,644 µm) produced by Krahn Chemie GmbH are used. Both powders are mixed into distilled water with a deflocculant Dolapix CE64 elaborated by Zschimmer & Schwarz GmbH, polyethylene

glycol PEG 400 from Merck GmbH as binder and Contraspum (Zschimmer & Schwarz GmbH) as antifoaming agent. After mixing, the samples are cast into gypsum moulds and cured at room temperature for 24 h. Then the removal of the ceramic pieces from the moulds can take place. The samples are dried at room temperature for further 24 h. The surfaces of each sample are ground to achieve a prismatic geometry (around 50 mm × 5 mm × 5 mm after sintering). The samples are sintered at 1550 °C for 3 h with a heating and cooling rate of 2 K/min. 10 samples of each formulation are cast.

The density of the samples are determined after sintering according to Archimedes principle in order to control eventual failure during the elaboration.

Thermal shocks in water are conducted on 5 samples of each formulation to guarantee representative values of elastic properties. Those quenching tests are conducted according to DIN 51068 at 400 °C [15]. The samples are dried after each thermal shock cycle before performing the measurements of the elastic properties. Three thermal shock experiments are conducted. As previously mentioned, this work highlights the ensuing elastic properties after the first thermal shock cycle.

2.2 The Impulse Excitation Technique (IET)

The elastic properties of each sample, namely the Young's modulus, the damping of the flexural resonant frequency and the non-linearity of the flexural resonant frequency are determined through Resonant Frequency Damping Analysis according to ASTM C 1548-02 with help of a testing device provided by IMCE/BE [16].

2.2.1 Young's modulus

As the sample geometry does not allow the acquisition of the torsion frequency, this study only focuses on the evolution of the flexural frequency. Therefore, the Poisson's ratio of each formulation is assumed to be similar after sintering and after thermal shock: a value of 0,20 is implemented in the calculation of the Young's modulus. In this technique, a specimen subjected to proper mechanical boundary conditions in accordance with the expected mode of vibration is excited by a short and light mechanical impulse in the middle of its lower surface once the sample is positioned on the sample holder as shown on Fig. 1. The acoustic response is sensed by a microphone and processed according to the frequency and attenuation rate detection. For bars with square cross-sections excited at the flexural mode of vibration, the Young's modulus (E) is calculated using the following equation:

$$E = 0{,}94642 * \left(\frac{m \cdot f_f^2}{b}\right) * \left(\frac{l}{h}\right)^3 * T \quad (1)$$

The parameter f_f is the flexural resonant frequency of the specimen (Hz), h is the specimen thickness perpendicular to the vibration direction, l is the specimen length, b is the specimen width and T is a geometrical correction factor that depends on the aspect ratio of the specimen (depending on l and h) and on the Poisson's ratio (supposed to equal to 0,20 in this study for each specimen). Three measurements are carried out on each sample to control the reproducibility of the measurement and to provide representative mean value of stiffness.

2.2.2 Damping of the flexural resonant frequency

The damping (δ) of the flexural resonant frequency is commonly calculated using the logarithmic decrement method:

$$\delta = \ln\left(\frac{x(t)}{x(t+T_d)}\right) \quad (2)$$

The parameter $x(t)$ is the amplitude of the sinusoidal signal decay function at time t, $x(t+T_d)$ is the amplitude of the same signal at time $t+T_d$ and T_d is the resonant frequency period. Damping property (δ) is dimensionless.

For a possible comparison of the results, the same experimental geometric conditions are considered. First of all, an automatic positioning sample holder is used to impose the mechanical boundary condition so that the flexural nodes could be predominantly excited. The distance between the microphone and the samples is kept to 5 mm. The excitation is delivered with help of an automatic hammer. To avoid any undesirable effects and to minimize eventual non-linearity acoustic response, the intensity of the impulse excitation is kept constant [17]. The sample holder apparatus used in a flexural mode can be seen in Fig. 1.

2.2.3 Non-linearity behaviour of the flexural resonant frequency

After processing, the acoustic response of each specimen can be split into several time frames and be considered as individual acoustic response. This tuning of the acoustic signal is provided by an extra non-linearity module also supplied by IMCE/BE. Each elastic property, namely flexural resonant frequency and its respective damping behaviour, can be determined in each time frame composing the whole acoustic signal response.

The size of the measurement window (time frame) and the size of the measurement step are kept constant for a possible results comparison. Within this framework, parameter α is defined to illustrate the non-linear behaviour of the flexural resonant frequency and is defined as the ratio between the flexural frequency in the time frame i divided by the property in the

Fig. 1 a) Flexural mode experimental set up for the determination of elastic properties; b) overview of the measuring principle and the tested sample geometry (sample based on 50 % Al_2O_3 and 50 % ZrO_2)

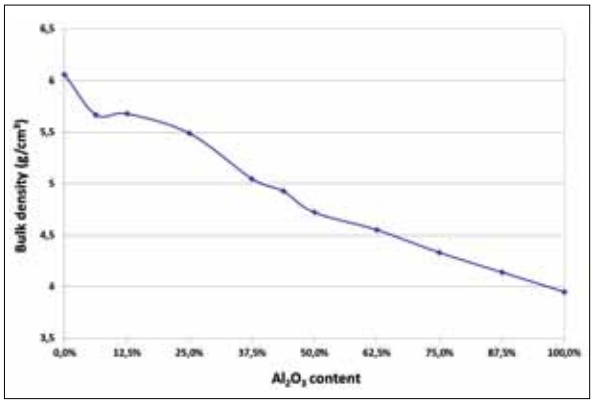

Fig. 2 Evolution of the bulk density of the tested formulations according to the alumina content

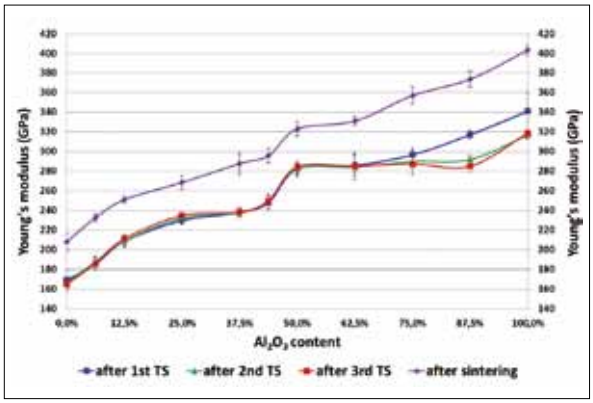

Fig. 3 Evolution of the retained Young's modulus of tested formulations in function of the alumina content after progressive thermal shock cycles

beginning of the time sinusoidal decay function, where the amplitude of the signal is the highest.

$$\alpha = \left| \frac{fr_{Amp_i}}{fr_{Amp_{max}}} \right| \quad (3)$$

The parameter $fr_{Amp\ i}$ represents the value of the flexural frequency of the peak point in the time sinusoidal signal decay function and $fr_{Amp\ max}$ represents the value of the frequency of the peak point in the time sinusoidal signal decay function with the maximum amplitude. Like damping, non-linearity parameter α is dimensionless.

3 Results and discussions

3.1 Bulk density

In order to avoid manufacturing failures, such as inclusions or undesirable mistakes by weighing, could influence the stiffness properties of the samples, the bulk density of each formulation is determined according to Archimedes' principle (DIN EN 993-1) [18]. The evolution of the bulk density of each tested formulation according to the alumina content is shown on Fig. 2. A linear evolution can be observed with addition of alumina and the achieved experimental bulk density values are close to the theoretical ones with for the formulations based on alumina and on partially stabilised zirconia. This linear behaviour may consequently guarantee an interpretation of stiffness evolution according to the nature of the formulation depending only on the raw materials and the contact surface between zirconia and alumina particles.

3.2 Young's modulus

Fig. 3 shows the stiffness evolution of the tested formulations up to the third thermal shock cycle. Once again, a linear behaviour with regard to the sample stiffness is noticeable after the sintering with addition of alumina and the achieved Young's modulus values are close to the theoretical ones with 403,4 GPa for the formulation based on alumina and 208,2 GPa for the formulation based on zirconia. It is worth mentioning that the Young's modulus value of the formulation containing 50 % alumina and 50 % zirconia deviates substantially from the trend line, while no impact of the elaboration process can be revealed through bulk density measurements.

After the first thermal shock cycle, the Young's modulus values of each formulation decreased as expected. However this decrease seems to be similar for each formulation. Therefore, a parallel evolution of the stiffness is observed. In other words: Such thermal shock conditions do not lead to conclusions about the relevance of partially stabilised zirconia use with regard to thermal shock resistance improvement. The successive thermal shock cycles do not influence the retained modulus of elasticity of the formulation up to a minimum alumina content of 62,5 % as the Young's modulus values remain unchanged in the alumina content range 0–62,5 %. Nevertheless, the stiffness of the formulations containing 75 %, 87,5 % and 100 % alumina keeps on slightly decreasing. In such experimental conditions, a minimum zirconia content of 37,5 % can be supposed to be beneficial against microstructural damaging.

3.3 Damping behaviour

As expected, the damping values of tested samples after the sintering are low, as only friction mechanism at the grain boundary of alumina and zirconia particles can take place in such a dense microstructure. Those damping values follow the inverse tendency of the Young's modulus. The lower the Young's modulus, for the formulation based on zirconia, the higher the damping behaviour with a value of $7{,}5 \cdot 10^{-4}$. And conversely, the higher the Young's modulus, as far as the formulation based on alumina is concerned, the lower the damping behaviour with a value of $1{,}9 \cdot 10^{-4}$. Thus it can be assumed that friction phenomena are more considerable at the interfaces between zirconia particles than those that can take place at the level of the interfaces between alumina particles and between alumina and zirconia particles.

Despite a similar decrease of the stiffness of each formulation after the first thermal shock cycle, the damping behaviour of those formulations does not follow the same trend as shown on Fig. 4. Indeed, a strong decrease of the internal friction is noticeable up to an alumina content of 25 % from $4{,}9 \cdot 10^{-3}$ for the formulation based on zirconia to $1{,}7 \cdot 10^{-3}$ for the formulation containing 25 % alumina and 75 % zirconia. As for the formulations containing more alumina are concerned, the damping values are quite constant and are contained in a range from $1{,}6 \cdot 10^{-3}$ to $2{,}3 \cdot 10^{-3}$. The internal friction phenomena between alumina particles and zirconia particles in presence of a crack network seem to be enhanced in an environment rich in zirconia with a

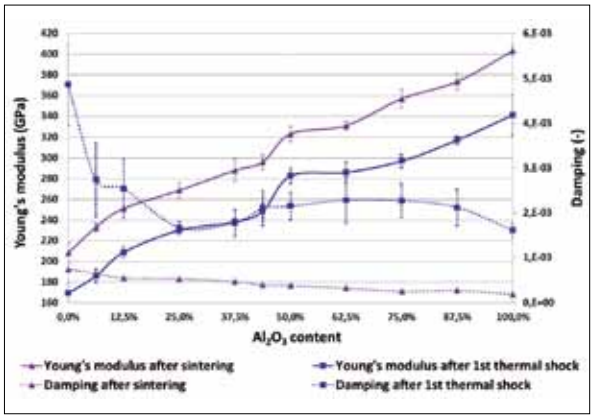

Fig. 4 Evolution of the Young's modulus and the damping behaviour of the tested formulations after the first thermal shock cycle

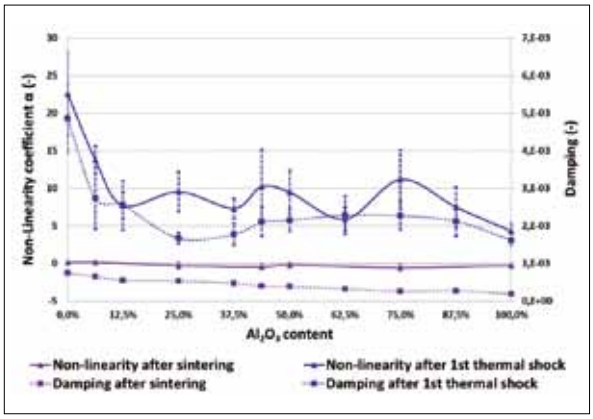

Fig. 5 Evolution of non-linearity of the flexural resonant frequency and damping behaviour evolution after the first thermal shock cycle

minimum content of 75 % of zirconia. Friction between zirconia particles can be subsequently considered as major sources of damping in comparison with friction that could take place at the interfaces between alumina particles or between alumina and zirconia particles.

3.4 Non-linearity of the flexural resonant frequency

Like damping, the non-linearity of the flexural resonant frequency is also sensitive to the presence of cracks. After sintering and as shown in Fig. 5, the non-linearity behaviour of each formulation can be reduced to zero values. That proves the low crack density in the microstructure of each formulation after the sintering. By supposing a more considerable sensitivity against cracks as far as the non-linearity is concerned, it is worth mentioning that the friction mechanisms occurring at the grain boundaries can be revealed through damping measurements and not through the examination of the non-linearity behaviour. After the thermal shock treatment, the evolution of the non-linearity coefficient follows the same trend as the damping behaviour. Indeed, a drastic decrease of the non-linearity coefficient is noticeable up to an alumina content of 12,5 % from 22,6 for the pure zirconia based formulation to 7,7 for the formulation containing 12,5 % of alumina and 87,5 % of zirconia. Concerning the formulations containing more alumina, the values of the non-linearity coefficient remain quite constant and vary from 5,9 to 11,2. The presence of cracks at the interfaces of zirconia particles may have a stronger influence on the non-linear behaviour of the acoustic signal than the cracks propagating at the grain boundaries of alumina particles or the cracks separating zirconia and alumina particles.

3.5 Microstructure examination

To better understand the damping behaviour of the Al_2O_3–ZrO_2 system, and more particularly after crack generation through thermal shock experiments, an accurate examination of the interfaces in contact with the cracks is needed to be carried out. Indeed, according to the nature of the formulation, three different kinds of contact surfaces can be created: alumina/alumina, alumina/zirconia and zirconia/zirconia. Starting from this statement, the examination of the microstructure leads to a better understanding of both crack configuration and nature of the interfaces.

Fig. 6–7 give an overview of the microstructural damage after thermal shock test of samples based on pure alumina and on

Fig. 6 Overview of microstructural damaging of sample based on pure alumina after thermal shock test in water

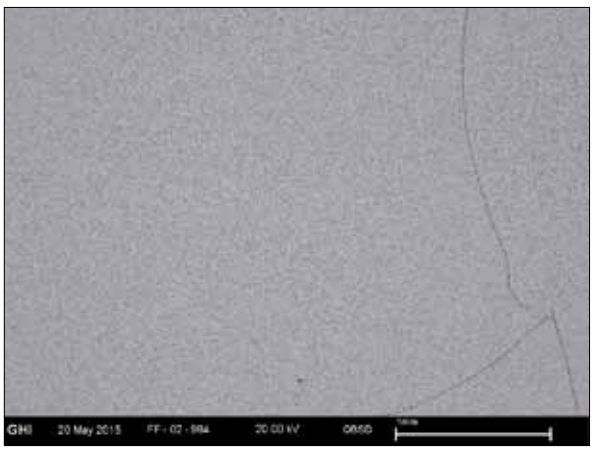

Fig. 7 Overview of microstructural damaging of sample based on 6,25 % alumina and 93,75 % zirconia after thermal shock test in water

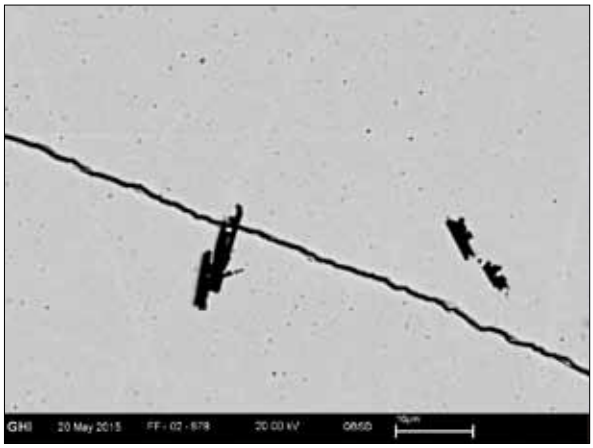

Fig. 8 Crack crossing over a pore in a pure zirconia sample after thermal shock test in water

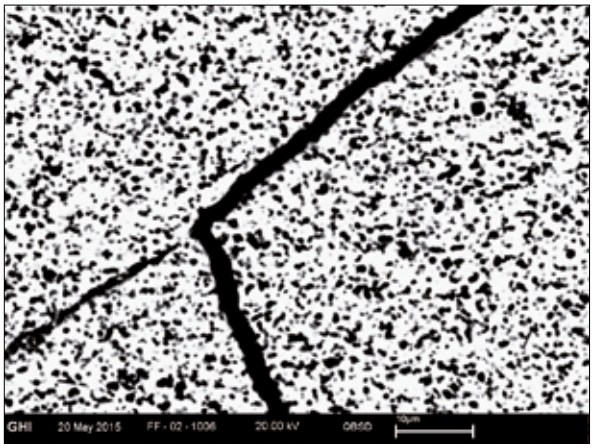

Fig. 9 Crack propagating throughout the matrix of a sample based on 25 % alumina and 75 % zirconia after thermal shock test in water

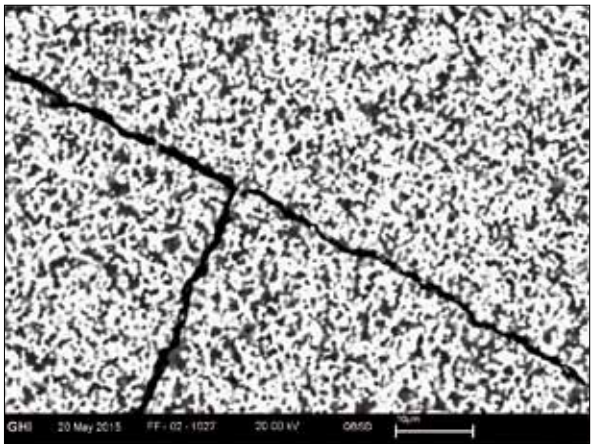

Fig. 10 Crack branching or crack unification in the matrix of a sample based on 50 % alumina and 50 % zirconia after thermal shock test in water

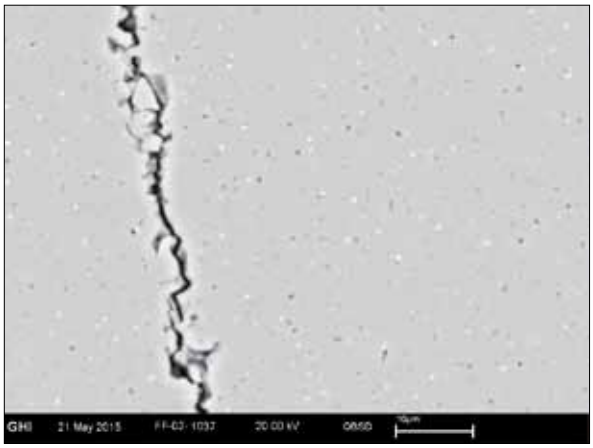

Fig. 11 Crack propagation throughout the matrix of a pure alumina sample after thermal shock test in water

6,25 % alumina and 93,75 % zirconia. Both samples exhibit a similar crack density and such a crack density can be observed in all tested materials of the Al_2O_3–ZrO_2 system. This microstructural examination is in agreement with the comparable stiffness decrease observed for each sample after the first thermal shock cycle. In both samples, cracks propagate throughout the matrix and thoroughly across the sample. In both cases, the crack path is straight on and a crack branching can be observed in case of the sample based on 6,25 % alumina and 93,75 % zirconia. Nevertheless, the crack network present in the pure alumina sample does not appear so clearly as the one of the sample based on 6,25 % alumina and 93,75 % zirconia. The further examination of the microstructure will show a discrepancy with regard to the crack width between the sample only containing alumina with a small crack width and the samples containing zirconia characterized by a higher crack width. To better understand the damping and non-linear behaviours of the tested samples, an accurate examination of the local microstructure surrounding the crack is required. Fig. 8–11 show in more detail the interfaces between cracks and the neighbouring particles of tested samples of the Al_2O_3–ZrO_2 system after quenching test in water.

A first observation will consist in focusing on microstructural part, which is not damaged. It is worth mentioning that the samples with a high content of zirconia (above 25 %) present a characteristic platelet-like pore structure with a length of around 10 µm and a width of around 3–5 µm in addition to spherical pores that could be found in any sample with a diameter under 1 µm. The presence of such pores can also explain the higher damping values after sintering of the samples with a high content of zirconia. Indeed, by exciting such samples, some internal friction can take place at the level of those elaboration defects. Besides the considerable friction between zirconia particles, the higher defect density is responsible for damping behaviour enhancement.

Considering the damaged areas of the microstructures, it is noticeable to conclude to an influence of the nature of the phase on the crack network. The samples containing more than 25 % of zirconia present the same crack configuration. Those cracks are propagating straight on throughout the microstructure and the distance between the crack flanks remain the same in the whole crack length. This crack width is in-

dependent of the content of zirconia and lies around 1–3 µm. The cracks surface is so smooth, that trivial friction phenomena between two flat surfaces can be considered. Concerning the samples rich in alumina (with an alumina content above 75 %), the cracks have a saw-tooth profile and an interlocking microstructure can be observed. The random granular stacking at the level of the cracks may be at the origin of more probable friction phenomena after excitation of the sample.

4 Conclusions

Thermal shock experiments are performed on formulations of the Al_2O_3–ZrO_2 system according to DIN 51068 at 400 °C. The study of the microstructure of those formulations leads to a correlation between microstructural damage and elastic properties, namely the Young's modulus, damping behaviour and non-linearity of the acoustic response.

Bulk density measurements after sintering show a linear evolution in the whole Al_2O_3–ZrO_2 system. It can be assumed that the tested samples present no defect due to the elaboration and subsequently the evolution of the elastic properties can be explained by the lonely nature of the phase. Nevertheless, typical platelet-like pores are found in the microstructure of samples with a high content of zirconia. Such pores may also contribute to the increase of the damping behaviour.

The retained Young's modulus measurements show a similar decrease of the stiffness, as the Young's modulus of the tested formulations follow the same tendency of evolution before and after thermal shock. As expected, the Young's modulus values after thermal shock decrease because of crack initiation in the microstructure. This similar decrease reveals a similar crack density in each tested sample. That can be verified by the examination of the microstructure overview of the samples after thermal shock. Therefore, the evolution of the damping behaviour and of the non-linearity of the acoustic response can be interpreted by the examination of the configuration of the crack network. The following thermal shock cycles do not have any impact on the stiffness of the material expected for the formulations with a content of alumina above 62,5 % where a low decrease of the stiffness is observed. It can be assumed that the stored elastic energy of those samples rich in alumina is so high that a lonely thermal shock cycle at 400 °C is not enough to release this stored elastic energy.

The damping behaviour of the tested materials of the Al_2O_3–ZrO_2 system, regarded as a tribological property, has to be interpreted by taking into consideration the crack geometry and especially the crack width, and the nature of the phases present at the interfaces. For formulations with a zirconia content above 75 %, despite the presence of cracks propagating straight on throughout the microstructure and a constant crack width in the whole crack length, the friction phenomena between zirconia particles is predominant and explain the high damping level. For formulations with a zirconia content between 25 % and 75 %, a same crack configuration is observed as the previous one. For such compositions, the interfaces between alumina particles and zirconia particles are predominant. In this context, friction is not so considerable as between zirconia particles. This explains the constant and low damping values. As far as the formulations rich in alumina are concerned, the contact between alumina particles is predominant and should be the scene of lower friction phenomena. The damping values of those compositions should be lower. However, in that case, the crack configuration is different. The ensuing interlocking structure favours those friction phenomena and is responsible for a higher contact surface between the crack flanks for the same crack density. That explains the damping values of formulations rich in alumina, which are almost as high as those of the formulations of the system 25 %–75 % zirconia.

The non-linear acoustic response turns out to be strongly correlated with the microstructural and physical properties, which influence the damping behaviour of the specimen. Even if studies tend to show the sensitivity of this propriety and the dependence of the crack density on this parameter, it has been shown through thermal shock tests that the non-linear acoustic response varies in function of the crack configuration and the nature of the phases present at the crack surfaces.

Acknowledgements

The authors would like to express their sincere thanks to the Ciência sem fronteiras (Science Without Borders) scholarship program founded by CAPES in cooperation with DAAD (German Academic Exchange Service) for the financial support of both students Gabriela Diniz Franca and Pierluigi Piccolo, who have performed the experiments of the survey.

References

[1] Miyaji, D.Y.; Tonnesen, T.; Rodrigues, J.A.: Fracture energy and thermal shock damage resistance of refractory castables containing eutectic aggregates. Ceramics Int. **40** (2014) [9] Part B, 15227–15239

[2] Boccaccini, D.N.; et al.: Determination of thermal shock resistance in refractory materials by ultrasonic pulse velocity measurement. J. Europ. Ceram. Soc. **27** (2007) [2–3] 1859–1863

[3] Aly, F.; Semler, C.E.: Prediction of refractory strength using non-destructive sonic measurements. Amer. Ceram. Soc. Bull. **64** (1985) [12] 1555–1558

[4] Mignard, F.; Olagnon, C.; Fantozzi, G.: Acoustic emission monitoring of damage evaluation in ceramics submitted to thermal shock. J. Europ. Ceram. Soc. **15** (1995) [7] 651–653

[5] Luz, A.P.; et al.: Thermal shock damage evaluation of refractory castables via hot modulus measurements. Ceramics Int. **39** (2013) [6] 6189–6197

[6] Tonnesen, T.; Telle, R.: Thermal shock damage in castables: Microstructural changes and evaluation by a damping method. cfi/Ber. DKG **84** (2007) [9] E132–E136

[7] Chen, R.Z.; Tuan, W.H.: Toughening alumina with silver and zirconia inclusions. J. Europ. Ceram. Soc. **21** (2001) [16] 2887–2893

[8] Mamivand, M.; Zaeem, M.A.; El Kadiri, H.: Phase field modeling of stress-induced tetragonal-to-monoclinic transformation in zirconia and its effect on transformation toughening. Acta Materialia **64** (2014) 208–219

[9] Fruhstorfer, J.; et al.: Microstructure and strength of fused high alumina materials with 2.5 wt-% zirconia and 2.5 wt-% titania additions for refractory applications. Ceramics Int., available in press (2015)

[10] Roebben, G.; et al.: Transformation-induced damping behaviour of Y-TZP zirconia ceramics. J. Europ. Ceram. Society **23** (2003) [3] 481–489

[11] Pasaribu, H.R.: Friction and wear of zirconia and alumina ceramics doped with CuO. University of Twente, Enschede 2005

[12] Hasselman, D.P.H.: Unified theory of thermal shock fracture initiation and crack propaga-

tion in brittle ceramics. J. Amer. Ceram. Soc. **52** (1969) 600–604

[13] Duck, F.A.: Nonlinear acoustics in diagnostic ultrasound. Ultrasound in Medicine and Biology **28** (2002) [1] 1–18

[14] Abeele, K.V.D.; Visscherb, J.: Damage assessment in reinforced concrete using spectral and temporal nonlinear vibration technique. Cement and Concrete Research **30** (2000) 1453–1464

[15] DIN 51068: Determination of resistance to thermal shock – Water quenching method for refractory bricks, 2008

[16] ASTM C 1548-02: Standard test method for dynamic Young's modulus, shear modulus, and Poisson's ratio of refractory materials by impulse excitation of vibration. ASTM International (2007)

[17] Traon, N.; Tonnesen, Th.; Telle, R.: Comparison of the elastic properties determined by different devices in a refractory castable based on partially stabilised zirconia. Proc. 53rd Int. Coll. on Refractories, Aachen 2010, 98–101

[18] DIN EN 993-1: Method of test for sense shaped refractory products – Part 1: Determination of bulk density, apparent porosity and true porosity, 1995